

Utilization of Jute Waste for Sustainable Eco-Film Preparation

Khairul Islam, Tarikul Islam,* Md. Nura Alam Shiddique, Manindra Nath Roy, Md Fahimuzzaman, Md. Azharul Islam, M Mahbubul Bashar,* and Mubarak A. Khan

Cite This: *ACS Sustainable Resour. Manage.* 2024, 1, 517–529

Read Online

ACCESS |



Metrics & More



Article Recommendations



Supporting Information

ABSTRACT: Jute caddis is the waste lignocellulosic biomass produced from jute fabric (sacking and hessian) production. Jute caddis cellulose (JCC) is a sustainable source and has high potential for being used in preparing biodegradable films. In this research, flexible, semi-transparent, biodegradable, and highly water-resistant eco-films were developed with cellulose extracted from JCC. The macroscopic cellulose was isolated from JCC by alkaline hydrolysis. Flexible and translucent cellulose films were produced with different amounts of JCC by vacuum filtration. Biodegradable thermoplastic polyurethane (TPU) was self-assembled and heat-pressed to fabricate semi-transparent films. The prepared eco-films were investigated using modern techniques for their mechanical properties, structural changes, thermal stability, and water resistance. With full flexibility (folding tolerance >100), the tensile strength of the JCC films was higher than that of low-density polyethylene (LDPE) films. The tensile strength of the TPU-coated JCC films was about 4 times higher than that of the pristine uncoated films. The films showed excellent water resistance, indicating a water contact angle higher than 100°, and the water droplet was found to be stable even after 20 min. A burning test of the JCC films showed that they produced ashes like paper burning, suggesting easy and clean biodegradation. The fabricated JCC eco-films could be a sustainable approach for replacing fossil-fuel-based petroleum plastic materials for packaging applications.

KEYWORDS: *jute caddis cellulose, thermoplastic polyurethane, contact angle, biodegradability, eco-films, functional coating*



INTRODUCTION

The growing interest in edible plastics reflects a strong inclination toward sustainable alternatives, seeking to replace traditional non-environmentally friendly polymer packaging with environmentally friendly options. This alternative has the potential for widespread use and could significantly contribute to preventing climate change and fostering a healthier environment. Despite the affordability and versatile utility of non-environmentally friendly polymer film materials, such as thin polyethylene, there is a pressing issue of mismanagement, with an estimated 60–99 million metric tons of mismanaged plastic waste being produced globally per year, which is projected to increase to 155–265 million metric tons per year in the future.¹ This poses a serious threat to nature. In 2015, the world generated a staggering 6.3 billion metric tons of plastic waste. If this production rate persists without proper supervision, it could escalate to 12 billion metric tons by 2050, resulting in an annual economic loss of \$80 billion (about \$250 per person in the U.S.).^{2,3} Notably, environmentally harmful, unfriendly polymer packaging remains widely used due to its flexibility and comparatively low cost in contrast to eco-film polymer packaging, which, despite its flexibility, comes at a higher price. This cost disparity is a major impediment to its widespread adoption.⁴ Historically, researchers have tried to

reduce the cost of bioplastics by incorporating thermoplastic polyurethane (TPU)⁵ or carboxymethyl cellulose (CMC)⁶ with natural resources such as starch,⁷ lignocellulose,⁸ and cellulose.⁹ However, an innovative approach involving the combination of CMC, TPU, and jute fiber caddis has not been explored to enhance biodegradability and reduce costs.

Jute caddis, the predominant industrial waste in the jute sector, constitutes 6–8% of the total jute consumption in the mills. Annually, Bangladesh produces 1.6 million t of jute fiber, and India produces 1.968 million t, with jute caddis accounting for approximately 0.3 million t in jute mills. Unfortunately, these caddis are commonly discarded, used as fuel in boilers, or treated as waste material, contributing to severe environmental damage.¹⁰ Proximate analysis of jute caddis reveals volatile matter at 58.6–65.0%, cellulose at 13.5–21.5%, hemicellulose at 11.5–14.0%, lignin at 11.5–14.0%, pectin at 0.2–0.4%, wax

Received: December 8, 2023

Revised: February 22, 2024

Accepted: February 23, 2024

Published: March 6, 2024



at 0.5–0.9%, moisture at 12.0–14.0%, and JBO and starch at 0.5–1.0%.^{11–16} Cellulose, a ubiquitous organic compound, is abundantly found worldwide. As the most prevalent biopolymer, it is natural and sustainable, derived from cultivated bast fiber and forest biomass remnants. Cellulose is an essential component of plant cell walls, playing a crucial role in maintaining the rigidity and strength of plants over time.¹⁷ Approximately 33% of all plant material is cellulose (cotton comprises 95%, and jute comprises 60–72%). Jute, cotton, and wood are the primary sources of cellulose used in industrial applications, notably in producing fabrics, sacking bags, paperboard, and paper.¹⁸

Mechanically, cellulose can be transformed into microcrystalline cellulose (MCC), which, when combined with CMC/TPU, becomes particularly valuable for creating water-resistant packaging in the food, cosmetic, and medical industries.¹⁹ The structure known as carboxymethyl cellulose (CMC) is the most significant configuration of polysaccharides. One of cellulose's crucial derivatives is CMC.²⁰ In CMC, carboxymethyl groups ($-\text{CH}_2-\text{COOH}$) or sodium carboxymethyl groups ($-\text{CH}_2\text{COONa}$) replace some of the hydroxyl (OH) groups of the glucopyranose units, typically at C2 > C6 > C3, resulting in a global output of 583.782 tons each year.²¹ CMC, a semi-crystalline chemical, can produce highly water-soluble, non-toxic, affordable, and biodegradable films with excellent film-building capabilities.⁸ Additionally, CMC finds diverse applications in food packaging,²² personal care products,²³ medicines, textiles,²⁴ fabrications,²⁵ papers,²⁶ adhesives, and ceramics.²⁷ It is in high demand in the scientific, industrial, and commercial sectors.²⁶ However, a drawback of CMC is its limited protection against deterioration, microbes, or sunlight.²⁸

The key properties of TPU include outstanding abrasion resistance, good mechanical properties with rubber-like flexibility, tear resistance, biodegradability, widespread availability, low cost, and super-transparency.^{5,29–31} Polyols and isocyanates constitute the main elements of polyurethane, where the isocyanate active group (NCO) reacts with the hydroxyl group (OH) present in jute caddis cellulose (JCC) through heat and pressure.³² TPU has been reinforced with natural fibers such as hemp, kenaf, sugar palm, oil palm empty fruit bunch, rice husk, hardwood core, and sisal.^{33–35} Synthetic fibers like glass, aramid, and carbon fibers have also been used for TPU reinforcement.^{35–37} In recent laboratory research, TPU has been reinforced exclusively with eco-friendly fibers.³⁸ Various attempts have been made to combine CMC, TPU, and polyvinyl alcohol (PVA) individually with jute fiber to create eco-friendly plastic packaging. These efforts have taken different approaches, including composites based on various TPU or CMC molecular weights and degrees of hydrolysis,^{21,39} composites using exceptionally fine jute and natural cellulose powder,^{6,40} and comparisons between composites prepared from both fine and coarse jute and natural cellulose powder.

However, none of these applications fully replicate the flexibility and transparency offered by non-environmentally friendly plastics, crucial attributes for real-world applications, such as malleable packaging for food, household items, and papers. The issues of hydrophobicity and the eco-friendliness of packaging made of TPU or CMC remain unanswered in the mentioned applications. While two recent studies have shown some improvements in the water resistance and eco-friendliness of films made with CMC and TPU, there have been no

sustained reports over time.²⁰ To bring JCC/TPU closer to commercial viability in eco-friendly flexible packaging, this research addressed four key questions: total flexibility, water resistance, transparency, and eco-friendliness. This study focused on four main aspects: (a) investigating the features of eco-friendly JCC/TPU packaging to achieve complete flexibility; (b) examining the influence of a water-resistant coating on the features of flexible JCC/TPU eco-friendly packaging; (c) analyzing transparency concerning the features of flexibility and water resistance in JCC/TPU eco-friendly packaging; and (d) studying eco-friendliness concerning the features of flexibility, water resistance, and transparency of JCC/TPU eco-friendly packaging.

Moreover, adhering to eco-friendly fabrication, this research employed a pure fabrication approach to minimize the waste produced throughout the procedure. Consequently, an eco-friendly packaging film was developed in this work using different ratios of JCC/TPU. The study observed and discussed modifications in the morphology, chemical structure, elemental analysis, thermal properties, mechanical properties, contact angle, air permeability, optical transmittance, and biodegradability of the eco-packaging film.

MATERIALS AND METHODS

Materials. Jute caddis (JC) was obtained from Bangladesh Jute Mills Ltd. (Ghorashal, Palash, Narsingdi, Bangladesh). Carboxymethyl cellulose (Grade P62), a sodium salt commonly known as sodium carboxymethyl cellulose (CMC), was procured from USK Kimya A.S. (Turkey). TPU granules and film were acquired from Xingxia Polymer Ltd. (Suzhou, China). Strong alkali (NaOH), hydrogen peroxide (H_2O_2), Rheopol BMW, Suntext XPA, Suntext UFB, Croaks NF, and acetic acid were purchased from Dysin-Chem Ltd. in Dhaka. All chemicals were of commercial grade, and acetic acid was utilized for neutralization.

Extraction of Jute Caddis Cellulose (JCC). Initially, jute caddis (2–3 mm) was cut into pieces using a jute cutter machine (model: GM800C) from Shandong Province, China, at Latif Bawany Jute Mills Ltd. (BJML), Bangladesh Jute Mills Corporation (BJMC), Bangladesh.⁴¹ Subsequently, the 1 kg JC pieces were boiled in a sample dyeing machine (Sclavos, Greece) for 3 h at 110 °C. The material-to-liquor ratio was maintained at 1:20 with 4.5 M strong alkali (NaOH), 0.5 M hydrogen peroxide (H_2O_2), 1 g/L Rheopol BMW, 1 g/L Suntext XPA, and 1 g/L Suntext UFB, and the pH was controlled at 10–11.⁴²

Following this treatment, the temperature was raised to 80 °C, and the pieces were boiled for 15 min with 0.25 g/L Croaks NF to neutralize the action of H_2O_2 . The resulting JCC was thoroughly washed in cold water.⁴³ Neutralization was achieved with 1 g/L acetic acid, followed by a second wash with cold water. The last step involved drying the washed JCC. It is worth noting that the ETP of BJ Mills Ltd. purified the water used in this process, which could be reused repeatedly.

Fabrication of JCC Powder. The JCC powder was produced by crushing the JCC at 35,000 rpm using an industrial herb powder pulverizer machine (ZT-1000, China) for 20 min to achieve a fine powder.⁴⁴ Subsequently, the JCC powder underwent sieving to attain a particle size of 0.2 mm (about 0.01 in.), as illustrated in Figure 1.

Fabrication of JCC Non-Woven Eco-Film. First, 1 g of CMC powder was stirred in a mixture of 0.2 L of distilled water at 500 rpm using a digital magnetic stirrer for 3 h at room temperature (20 °C) to achieve a homogeneous paste. Second, 6, 8, and 10 g of fabricated JCC powder was blended in a mixture of 1.8 L distilled water at 21,000 rpm using a Kiam mixer grinder (BL-1000, Bangladesh) for 10 min at room temperature (20 °C) to create a homogeneous pasting solution (see Table 1). Subsequently, the 0.2 L CMC paste was added to this solution, and it was remixed for 5 min at the same temperature to achieve a homogeneous cross-linking pasting solution. The JCC/

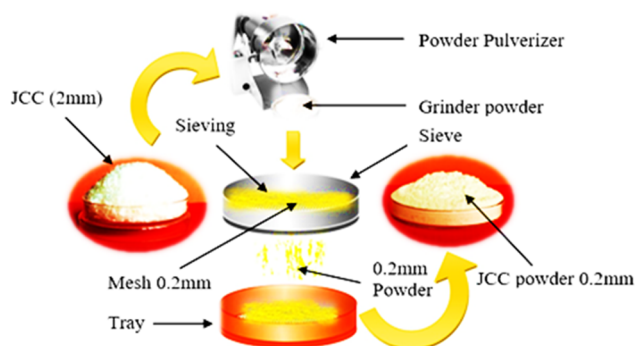


Figure 1. Fabrication of powder from jute caddis cellulose (JCC) using an industrial herb powder pulverizer machine.

Table 1. Sampling for the JCC and JCC/TPU Films

sample descriptions	identification
6 g of jute caddis cellulose (JCC)	JCC6
8 g of JCC	JCC8
10 g of JCC	JCC10
6 g of JCC + 0.30 g of thermoplastic polyurethane (TPU)	JCC6/TPU
8 g of JCC + 0.60 g of TPU	JCC8/TPU
10 g of JCC + 0.95 g of TPU	JCC10/TPU

CMC, JCC8/CMC, and JCC10/CMC pasting solutions were poured into a vacuum filtration system with overflow protection (see Figure 2) using nylon filter paper (diameter = 120 mm). The maximum

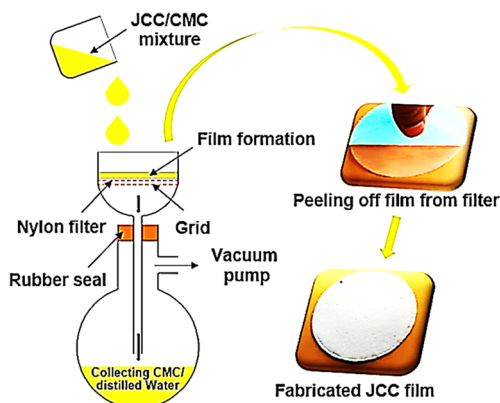


Figure 2. Method of fabricating jute caddis cellulose (JCC) non-woven fabricated film from the combination of JCC/CMC using a vacuum filtration arrangement.

CMC and total water were collected in the bottom beaker, while a white JCC film formed on the filter paper.⁴⁵ The films were then dried overnight in a vacuum oven (LabTech, Korea, model: LVO-2050) at room temperature. Finally, the films were peeled off of the filter paper.

Coating of JCC Non-Woven Fabricated Eco-Films by TPU. Initially, 2 g of TPU was dissolved in a 250 mL beaker containing 200 mL of acetone, and the mixture was covered with a Petri dish for 4 h. Subsequently, non-woven JCC6, JCC8, and JCC10 films were cut into 80 mm × 40 mm dimensions. These specimens were immersed in the TPU solution for 30 s, removed, and then hung to dry for 10 min at a temperature of 30 °C with 65% humidity. This immersion and drying process was repeated five times for each specimen. The resulting dried films were created from the TPU-coated transparent films by pressing them under 1 ton of pressure at 160 °C for 5 min using an Auto Series Plus press (Carver Inc., U.S., model: 4533.4FL1000). After this procedure, the remaining TPU was collected, and its weight was determined. In these specimens,

JCC6/TPU, JCC8/TPU, and JCC10/TPU contain 95%, 92.5%, and 90.5% JCC and 5%, 7.5%, and 9.5% TPU, respectively.

Characterizations. Morphology. The morphology of the JCC powder and the JCC/TPU-coated and uncoated JCC non-woven fabric films was examined using a scanning electron microscope (SEM) with a Zeiss Sigma 300 FEG instrument from Germany at an accelerating voltage of 15 kV. Before imaging, all fabricated films were coated with a 10 nm layer of gold using a Quorum Q150R S Plus sputter coater.⁴⁶ Subsequently, the films were analyzed by scanning electron microscopy, and images were collected for further analysis.

Fourier Transform Infrared Spectra. The chemical structure of the JCC powder and the JCC/TPU-coated and uncoated JCC non-woven fabric films was analyzed using Fourier transform infrared (FT-IR) spectroscopy. The measurements were obtained with a Spectrum Two spectrometer (PerkinElmer Inc., U.K.) over the 400–4000 cm^{-1} wavenumber range. The spectrometer had a scanning resolution of 4 cm^{-1} , and each specimen underwent four scans. For the analysis, the JCC powder, coated JCC/TPU films, and uncoated JCC non-woven fabric films were prepared into sheets measuring (10 × 10) mm. The sampling plate was cleaned with isopropyl alcohol, and the specimen was placed on the specimen plate. After the compression clamp was tightened, the scan was initiated using the software. The collected data were then analyzed, and graphs were generated using Igor Pro 6.04.

Thermal Properties. A thermogravimetric analyzer (model: TGA 4000, brand: PerkinElmer) was employed to assess the thermal properties of all specimens. Before testing, the specimens were dried in an oven at 60 °C for 8 h, and each specimen was then crushed into pieces weighing between 6 and 8 mg. Initially, the temperature was held at 50 °C for 1 min and then increased from 50 to 800 °C at a scanning rate of 10 °C/min. All experiments were conducted under a nitrogen flow of 20 mL/min.

Elemental Analysis of the Coated and Uncoated Eco-Films. The elements in the coated and uncoated films were analyzed by using an energy dispersive X-ray spectroscopy (EDS) system. Considering the chemical treatment applied to the specimens, the coated and uncoated films were selected as representatives for the elemental analysis. Before imaging, a 2 nm thick gold layer was coated onto the films by using a (Quorum Q150R S Plus) sputter coater. The results were then observed using a field emission scanning electron microscope (FESEM) with a Zeiss Sigma 300 FEG instrument from Germany, equipped with a detector operating at 10 kV. Images were collected for further analysis.

Mechanical Properties. The elongation at break, tensile strength, tensile index, and Young's modulus of both the coated JCC/TPU and uncoated JCC non-woven fabric films were determined using a universal tensile testing system (Fanyuan Instrument (HF) Co. Ltd., China). The testing system was equipped with a 1 N load cell, and the TAPPI/ANSI T494 standard testing method was followed. A constant elongation rate (10 mm/min) was applied during the measurements, maintaining a gauge length of 1 mm, and specimens were prepared with dimensions of 90 mm × 30 mm. A commercial, non-environmentally friendly packaging bag made of 60 μm of low-density polyethylene (LDPE) was also tested using the same method. Before measurement, all specimens were conditioned at 25 °C and 65% relative humidity. Three tests were conducted for each coated JCC/TPU and uncoated JCC non-woven fabric film, and the means with standard deviations were reported.

Thickness and GSM. The thickness of both the coated JCC/TPU and uncoated JCC non-woven fabric films was measured using a digital thickness meter (Sylvac, model: ISP091201D, Switzerland) with a measuring range of 150 mm, a contact point of $\varnothing 2/\text{M}2.5$ or 4-48-UNF, and an accuracy of 0.001 mm. Initially, the specimen was positioned on the plate of the thickness meter, and a reading was taken. Five readings were recorded for each specimen, and the average was calculated. Following this, the weight of each specimen was measured using a digital electric balance (model: JJ324BC, China) with a reading accuracy of 0.0001 g. The diameter of the specimen was determined using a scale, and the result was recorded. The GSM

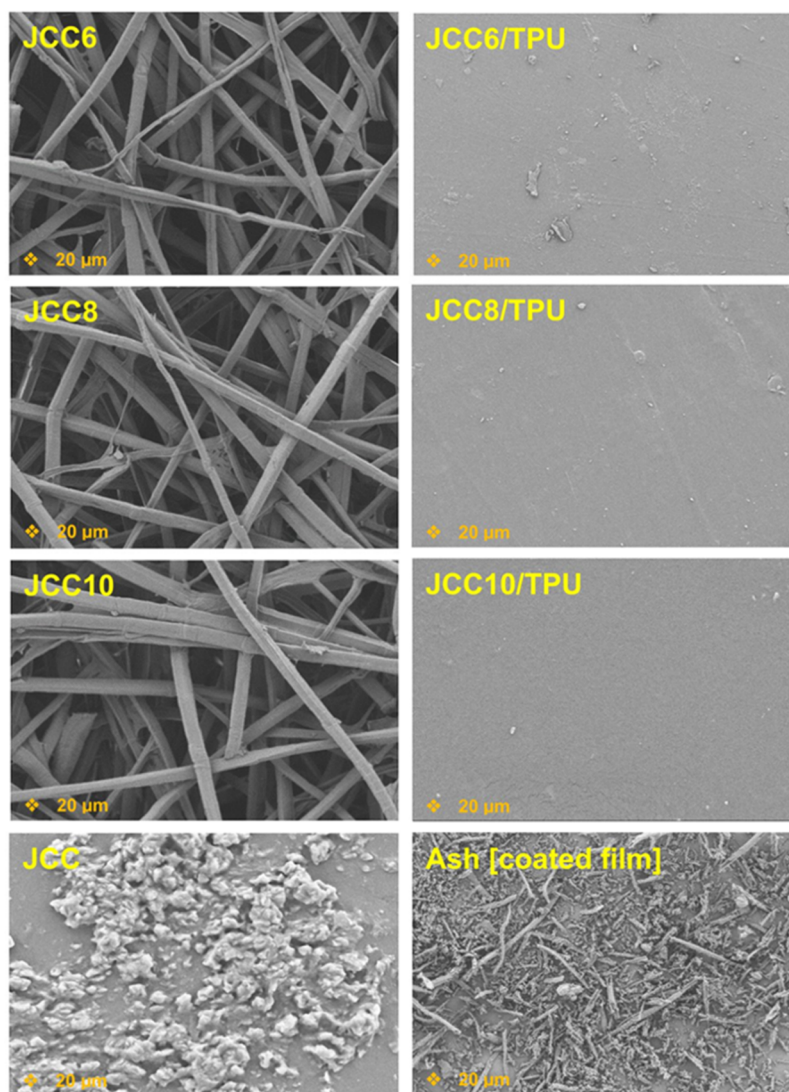


Figure 3. Scanning electronic microscopic (SEM) images of (left) the surface of JCC6, JCC8, and JCC10 uncoated films and JCC powder and of (right) the surface of JCC6/TPU, JCC8/TPU, and JCC10/TPU-coated films and ash of all corresponding coated films.

(grams per square meter) of the specimen was then calculated using eq 1:

$$\text{GSM} = \frac{4x}{\pi d^2} \quad (1)$$

where x and d are the weight and diameter of the sample, respectively. Each specimen was tested five times, and their mean and standard deviation values were recorded.

Sessile Water Drop Contact Angle. A Theta Lite optical tensiometer (Finland, model: Theta Lite-24830-05) was employed to evaluate the sessile water drop contact angle of both the coated JCC/TPU and uncoated JCC non-woven fabric films, along with the LDPE and TPU films. A sessile water droplet with a volume of 5.0 μL was applied to the film surface, and the mean value of the contact angles (both right and left) was automatically measured at intervals of 1, 15, 30 s, and 1, 5, 10, and 20 min at 10% (14 frames per second (FPS)). A common technique in analyzing film contact angles involves measuring the drop angle twice, once when the film is placed on the surface and again after 1 min;⁴⁷ this is considered the most accurate method. However, for this investigation, the test duration was extended to 20 min due to the need to assess water resistance. The results were presented at various time intervals, including those commonly used in practice (e.g., 1 s or 1 min)⁴¹ and those documented for water-resistant films (e.g., 10 min).⁴¹ This study

displayed the results at intervals of 1, 15, 30 s, and 1, 5, 10, and 20 min. The process was repeated three times for each film, and the mean values were utilized to generate the graph.

Air Permeability. The air permeability of the coated JCC/TPU and uncoated JCC non-woven fabric films was determined using an air permeability testing machine (Fanyuan Instrument (HF) Co. Ltd., China, model: YG461E). To ensure reliable results, the machine was calibrated before conducting the tests. In this evaluation, a circular specimen container with an area of 5 cm^2 was used, and the pressure was set at 100 Pa.³² Pressure drops across the specimen varied from 50 to 500 Pa. Wrinkles in the specimen were smoothed by applying adequate stress. The experiment was conducted at least five times in different areas of the specimen, and the results, including the mean and standard deviation, are presented here.

Biodegradability of Eco-Films. The biodegradation of the coated JCC/TPU and uncoated JCC non-woven fabric films was investigated in loamy soil within a flower garden at LBJML in Bangladesh. The films were cut into square shapes and buried in the garden soil with a pH of 7 (measured using a Hanna multi-parameter probe, U.S., model: HI7629829) for 120 days. At intervals of 20 days, the specimens were carefully retrieved, cleaned with water, dried, and weighed to assess weight loss (%) attributed to degradation. Additionally, another analysis involved a burning system.

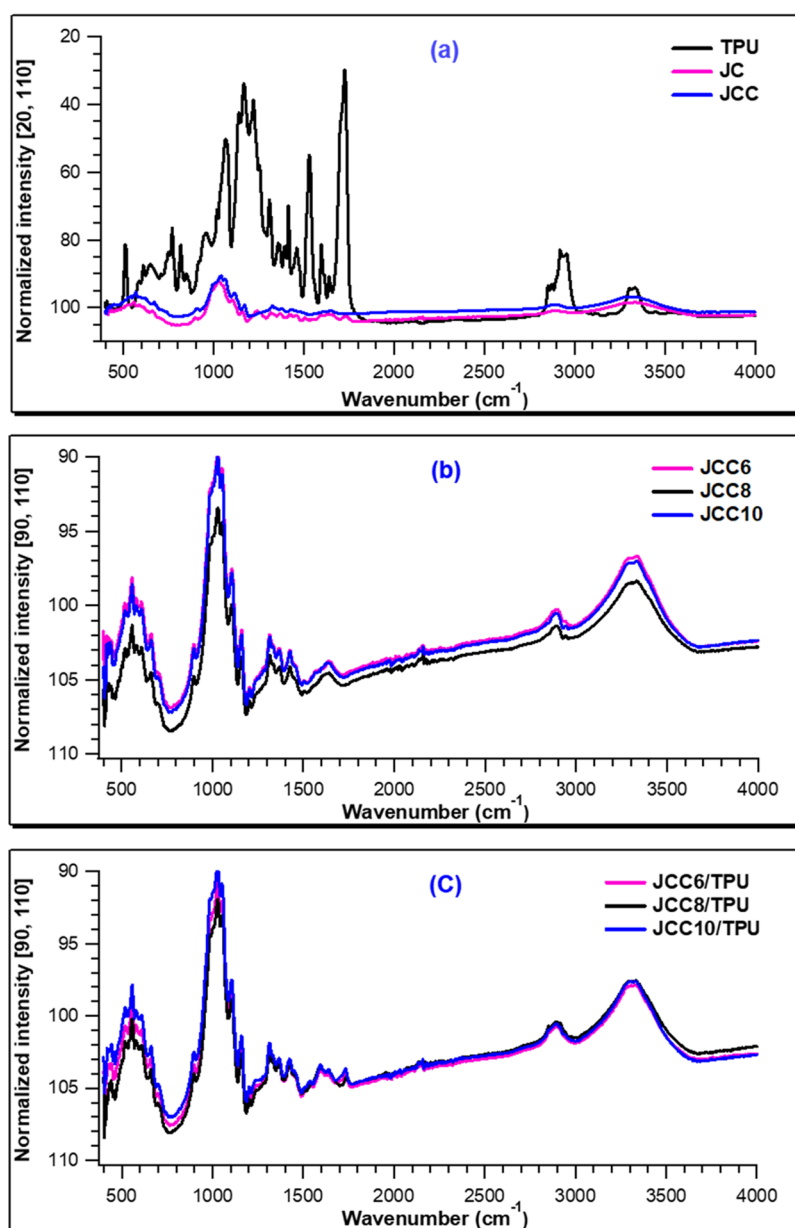


Figure 4. FT-IR spectra: (a) JC, JCC, and TPU; (b) uncoated JCC6, JCC8, and JCC10 fabricated eco-films; and (c) coated JCC6/TPU, JCC8/TPU, and JCC10/TPU fabricated eco-films.

RESULTS AND DISCUSSION

Morphology. SEM images of the ash from all corresponding coated films, JCC powder, and surfaces of both the coated and uncoated fabric films are presented in Figure 3. In this analysis, the JCC powder exhibited an almost spherical shape, resulting from cutting or grinding with a sharp, rounded steel knife, displaying a rough surface. The particle size of the ash obtained after the coated films were burned as fuel was $<1 \mu\text{m}$, with very few particles measuring $3 \mu\text{m}$, featuring rough surfaces. The non-woven fabric films produced from JCC contained large particles, notably rayon, which were entangled and ranged in width from 5 to $10 \mu\text{m}$. Despite differences in the thickness of the uncoated films for JCC6, JCC8, and JCC10, the surface roughness of these films was identical. Conversely, the coated film JCC10/TPU exhibited a smoother surface compared to JCC6/TPU. This difference may be attributed to the film thickness or the amount of JCC,

impacting other film properties like air permeability, contact angle, eco-friendliness, and light transmission, as discussed later. The TPU film displayed a comparatively smooth surface without any porosity.³¹ The influence of the TPU coating was evident on the surface of all coated films. This could result from the additional TPU coating covering the non-woven film, reducing the overall unevenness from JCC accumulation and increasing transparency. The morphology suggests that the adhesion and miscibility of JCC and TPU improve with heat and pressure, resulting in a smoother surface and higher transparency. Similar enhancements in the quality of CMC or starch-based films, such as the reduction of rough surfaces and improved smoothness⁴⁸ using TPU, have been extensively reported in the literature.

Chemical Structure. In the case of both the coated (JCC6/TPU, JCC8/TPU, and JCC10/TPU) and uncoated (JCC6, JCC8, and JCC10) fabricated films as well as JC and

Table 2. Characteristic Bands in FT-IR Spectra and Their Assignments and Functional Groups According to Literature Data

wavelength (cm ⁻¹)										functional group and assignments	ref
TPU	JC	JCC	JCC6	JCC8	JCC10	JCC6/TPU	JCC8/TPU	JCC10/TPU			
3346	3342	3340	3342	3335	3336	3334	3339	3335		intermolecular hydrogen bond and free OH groups and N-H vibration	49
3306	3284	3290	3290	3289	3292	3296	3296	3296			
2960	-	-	-	-	-	-	-	-		symmetric CH stretching	49
2920	-	-	-	-	-	-	2919	29120	2919	asymmetric CH stretching	49
-	2898	2898	2896	2895	2896	2899	2899	2899		symmetric CH stretching	49
2875	-	-	-	-	-	-	-	-		symmetric CH stretching	49
2851	-	-	-	-	-	2853	2851	2852		asymmetric CH stretching	49
1729	1736	-	-	-	-	1734	1737	1734		carboxylic groups (C=O) (ester or associated urethane)	50, 51
1643	1643	1643	1643	1643	1643	1643	163	1643		O-H (water absorption)	49
1598	-	-	-	-	-	1597	1597	1598		benzene group	51
-	1594	-	-	-	-	-	-	-		lignin components	49
1531	-	-	-	-	-	1535	1340	1535		N-H bending	51
-	1507	-	-	-	-	-	-	-		lignin components	49
1465	-	-	-	-	-	-	-	-		benzene group	51
-	1461	-	-	-	-	-	-	-		lignin components	49
-	1427	1428	1428	1428	1425	1426	1429	1428		-CH ₂ bending of pyranose ring	49, 52
1369	1371	1371	1371	1371	1370	1369	1371	1369		-CH bending and phenolic -OH	50
-	1317	1316	1317	1317	1315	1315	1316	1316		-CH ₂ bending in cellulose	49
-	1246	-	-	-	-	-	-	-		C-O stretching in lignin	49
1221	-	-	-	-	-	-	-	-		C-O-C stretching	51
1169	-	-	-	-	-	-	-	-		C-O-C stretching	51
-	1162	1162	1161	1161	1161	1160	1161	1161		C-O-C asymmetric stretching	49, 52
-	1106	1107	1107	1107	1107	1106	1105	1106		-CH in-plane deformation in aromatic ring	49, 52
-	1053	1053	1053	1053	1053	1053	1053	1053		C-O stretching in cellulose	49, 52
-	1031	1031	1030	1030	1030	1031	1030	1031		C-O/C-C stretching	50
-	895	896	894	899	898	896	898	890		BD-cellulose	50
770	-	-	-	-	-	-	-	-		C-O-O stretching	51

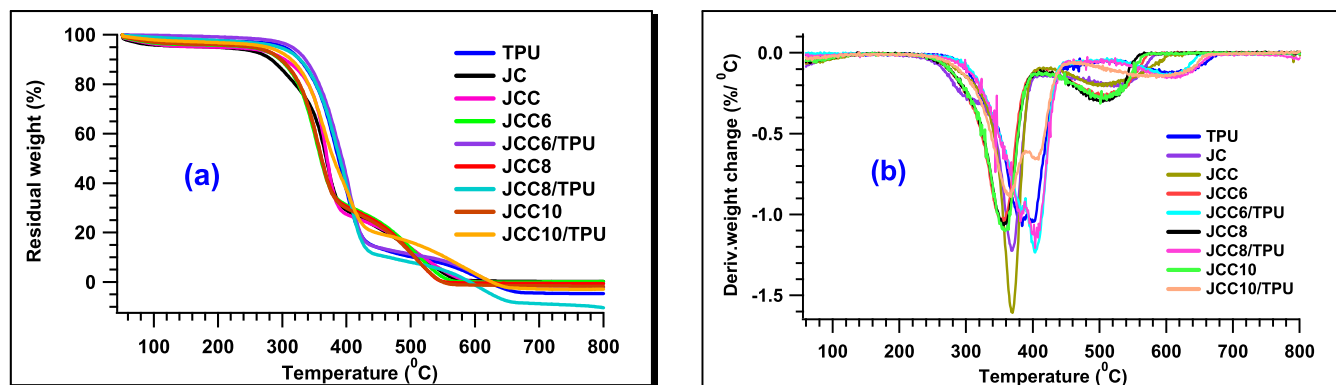


Figure 5. Thermal properties: (a) TGA and (b) DTG curves of JC, JCC, TPU, and the uncoated (JCC6, JCC8, and JCC10) and coated (JCC6/TPU, JCC8/TPU, and JCC10/TPU) eco-films.

Table 3. Thermal Properties of TPU, JC, JCC, and Coated and Uncoated Fabricated Films

specimen	$T_{5\%}$ (°C)	T_{onset} (°C)	T_{max} (°C)	weight (%) at temperature				
				300 °C	350 °C	400 °C	450 °C	500 °C
TPU	300	290	390	85.0	68.9	28.42	21.69	10.2
JC	150	250	370	85.6	67.5	28.9	21.7	13.34
JCC	230	270	370	90.5	74.2	27.4	22.1	13.53
JCC6	260	260	360	89.1	59.8	31.0	24.5	13.63
JCC8	260	260	360	89.5	61.0	30.5	23.7	11.92
JCC10	260	260	360	89.5	61.0	29.8	22.8	12.45
JCC6/TPU	310	280	400	96.7	83.9	42.0	13.9	15.2
JCC8/TPU	310	280	400	94.5	81.3	38.8	10.8	15.8
JCC10/TPU	290	280	400	92.43	73.99	36.96	19.45	15.28

Table 4. Distinct Phases of Weight Loss of JCC and Coated and Uncoated Fabricated Films Regarding Temperature Increase

specimen	weight loss (%)			residue (%)
	50–250 °C	250–420 °C	420–500 °C	500 °C
TPU	2.93	79.36	7.56	10.2
JC	5.57	63.44	17.65	13.34
JCC	5.57	65.63	15.27	13.53
JCC6	4.39	66.71	15.27	13.63
JCC8	4.30	67.39	16.39	11.92
JCC10	4.79	67.39	15.37	12.45
JCC6/TPU	4.5	74.35	5.95	15.2
JCC8/TPU	4.94	73.07	6.19	15.8
JCC10/TPU	4.82	72.62	6.52	15.28

JCC, similar peaks were observed, although different to those of TPU (see Figure 4). In TPU and the coated films, the peaks at 2960 and 2875 cm^{-1} for symmetric stretching vibrations and those at 2920 and 2851 cm^{-1} for asymmetric stretching vibrations are associated with functional groups from the C–H groups.⁵ The C–H stretching vibrations in JC, JCC, and the coated and uncoated films appear as sharp peaks around 2896–2899 cm^{-1} , confirming the presence of cellulose and hemicellulose.⁴⁹

Peaks near 1736–1729 cm^{-1} for C–O stretching indicate ester carboxylic groups in TPU for urethane or JC for hemicellulose, which disappear completely in JCC.⁵⁰ Peaks around 1643 cm^{-1} arise due to absorbed water in all specimens. Peaks at 1529 cm^{-1} are attributed to the stretching and bending of N–H bonds in urethane bonds, and the 1596 and 1470 cm^{-1} peaks are associated with a benzene group in TPU. Lignin components contribute to peaks in JC near 1594, 1507, and 1461 cm^{-1} , which disappear in JCC, indicating lignin removal. Peaks near 1429–1425 cm^{-1} can be attributed

to the CH_2 bending of the pyranose rings. The peak around 1316 cm^{-1} for CH_2 bending also indicates the presence of cellulose in JC, JCC, and the coated and uncoated films. Peaks around 1371–1369 cm^{-1} represent CH bending and phenolic OH stretching vibrations in all specimens. In JC, there is an intermediate peak near 1246 cm^{-1} due to C–O stretching in the ether linkage for lignin, but this peak disappears completely in JCC.⁵¹ Peaks around 1162–1160 cm^{-1} in JC and JCC are due to C–O–C stretching, confirming the presence of cellulose.⁵² Peaks around 1109–1107 and 1053 cm^{-1} represent vibrational C–O stretching and in-plane C–H deformation in all samples without TPU, and sharp peaks around 1031–1030 cm^{-1} correspond to C–O or C–C stretching.⁵⁰ The stretching vibrated in cellulose peaks near 1031–1030, 1053, 1107–1105, and 1162–1160 cm^{-1} .

Peaks near 898–890 cm^{-1} confirm the presence of the β -glycosidic linkage. The band near 1221 cm^{-1} is responsible for the C–O–C stretching of the urethane group,⁵¹ while the peak around 1169 cm^{-1} represents the C–O–C stretching of the ester group. Furthermore, the C–O–C stretching represents the urethane group for the peak at 770 cm^{-1} in TPU. In this investigation, the assignments of the FT-IR peaks for each sample are listed, and their respective functional groups, according to research, are presented in Table 2.

Thermal Stability of Coated and Uncoated Fabricated Films. The thermogravimetric analysis (TGA) and derivative thermogravimetric (DTG) curves of TPU, JC, JCC, and the coated and uncoated fabricated films are depicted in panels a and b of Figure 5, respectively. In this study, the thermal stability of TPU, JC, JCC, and the coated and uncoated films was analyzed through TGA, and the thermal resistance properties are presented in Table 3. Due to the presence of different functional groups, including carboxylic groups (C=O) in jute caddis (JC) and isocyanate active groups (NCO) in TPU, they contribute equally to

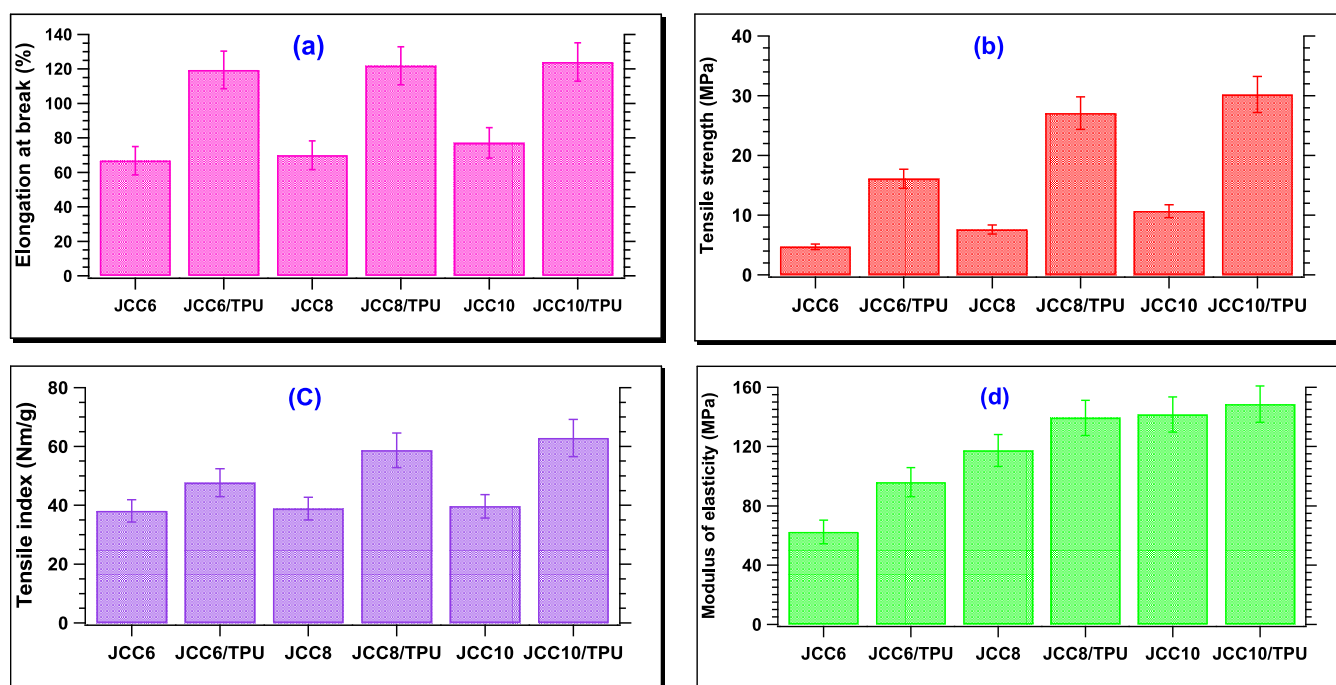


Figure 6. (a) Elongation at break, (b) tensile strength, (c) tensile index, and (d) modulus of elasticity of coated films JCC6/TPU, JCC8/TPU, and JCC10/TPU and uncoated films JCC6, JCC8, and JCC10 (different plots display data sets were different than others, i.e., $p \leq 0.5$).

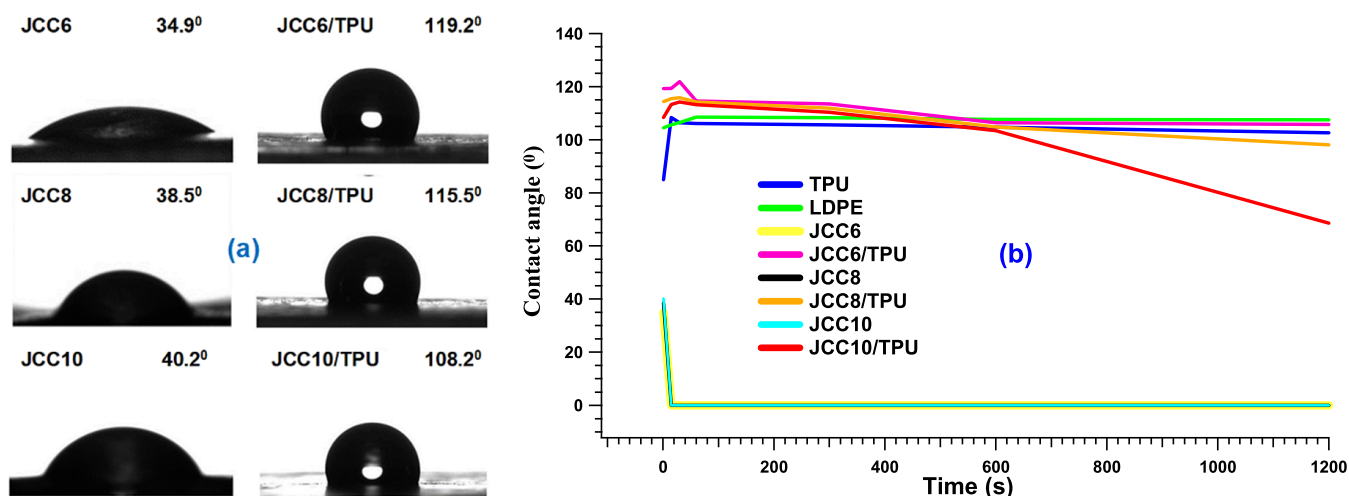


Figure 7. Sessile water droplet (a) images for 1 s and (b) contact angles up to 1200 s on the coated JCC6/TPU, JCC8/TPU, and JCC10/TPU and uncoated JCC6, JCC8, and JCC10 non-woven fabricated eco-films, TPU film, and low-density polyethylene (LDPE).

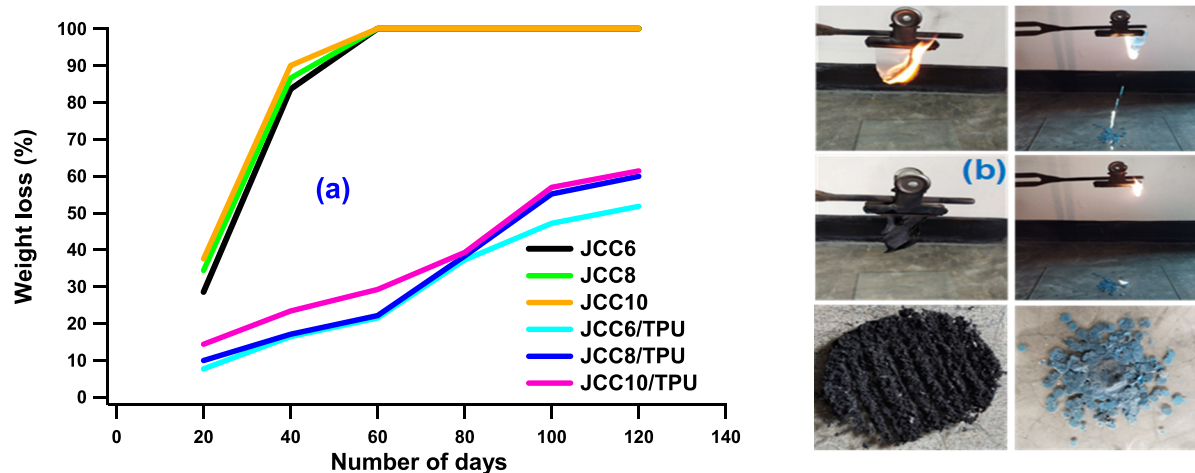


Figure 8. Weight loss of the coated JCC/TPU and uncoated JCC non-woven fabricated eco-films (a) prepared from jute caddis cellulose (JCC) due to biodegradation in soil, and (b) analysis by burning of the coated JCC/TPU eco-films and LDPE plastic.

decomposition. Usually, cellulose degradation is accompanied by depolymerization dehydration followed by the analogous decomposition of the glycosyl units of the cellulose chain, and this phenomenon can also occur in the case of JCC and the coated and uncoated films.⁴¹ Initially, moisture or oligomer evaporation was responsible for the first-stage degradation of all specimens at around 150 °C.⁵³ The decomposition of TPU, JC, JCC, and the uncoated and coated films began at 290, 250, 270, 260, and 280 °C, respectively. Similarly, the maximum decomposition temperature of the coated and uncoated films (respectively, 400 °C and 360 °C) was higher and lower than that of JC (370 °C), respectively, which may be due to them being coated with TPU and treated with NaOH. However, the temperature at a weight loss of 5% for JCC and the coated and uncoated films is about 100–150 °C higher than JC because JC contains low molecular weight non-cellulosic materials, which undergo faster decomposition.⁴¹

The DTG curves exhibited the three main flashpoints of weight change (%), as noted in Table 4. The first flashpoint was around 50–250 °C, associated with changes in moisture or oligomer evaporation,⁵⁴ for which none of the specimens showed a significant weight change (%). The second flashpoint was responsible for the decrease of most of the weight, which

occurred between 250 and 420 °C. This point of degradation in JC, JCC, and the coated and uncoated films can be related to the decomposition of hemicellulose and lignin⁵⁵ followed by cellulose. This could be explained by devolatilization reactions in which most of the organic component of all specimens was reduced as volatile matter. The proportion of the final phase weight change was found to be lower for all coated films and TPU compared to that of JC, JCC, and the uncoated films, which may be due the coated films being coated with TPU. This could be related to the excellent adhesion attribute of the coated films and better chemical cross-linking, which controlled the overall degradation ratio. This step of decomposition was completed at temperatures of around 420–500 °C. However, the residual weight change of the three different JCC/TPU-coated films was 15.2%, 15.8%, and 15.28%, respectively; these values were higher than those of their original elements, such as TPU, JC, and JCC, at the elevated temperature (>500 °C). The higher mass at the elevated temperature suggested the char formation ability of the coated films, which is one of the significant characteristics of the flame retardancy of the element.

Elemental Analysis of the Coated and Uncoated Eco-Films. The results of the EDS experiment for the coated and

Table 5. Comparison of Cellulose-Based Eco-Films According to Literature Data

fiber	mechanical properties					contact angle (deg)	transparency (%)	air permeability (L/m ² /S)	biodegradability %			ref
	elongation (%)	tensile strength (MPa)	Young's modulus (MPa)	tensile index (Nm/g)	tensile index (Nm/g)				40 days	80 days	120 days	
jute caddis (JC)	119.4–124.0	16.1–30.2	96.0–148.6	47.66–62.87	47.66–62.87	108.4–119.2	51.99–60.05	2.16–16.28	17.0–23.3	37.2–39.2	51.8–61.4	-
banana	5.8–5.9	27.5–45.6	811.8–1118.6	44.2–57.4	44.2–57.4	83.6	42.0–47.0	-	-	-	-	58
water hygienic	3.9–3.2	14.8–24.8	590.9–1017.3	28.8–32.8	28.8–32.8	72.4	38.2–47.2	-	-	-	-	58
cotton gin trash	11.1–25.1	20.1–27.1	340–1001	-	-	65	<50	-	-	-	-	57
hemp	-	-	-	-	-	51–90	-	-	20.0–24.5	70.0–80.0	90.0–100.0	60
seaweed	20.14–23.14	13.59–35.66	116–206	-	-	41.35–68.12	-	-	41.40–46.58	-	-	61

uncoated eco-films represent that both the coated and uncoated fabricated eco-films exhibited ten distinct elements, including carbon (C), oxygen (O), nitrogen (N), silicon (Si), potassium (K), calcium (Ca), aluminum (Al), sulphur (S), magnesium (Mg), phosphorus (P), and chlorine (Cl), except for gold (Au) due to the gold coating.⁴⁴ The amounts of these components slightly varied when analyzed in films of the two different properties (see Figure S5).

As the coated and uncoated films are lignocellulosic elements, in this investigation, C was found to be the major component in the coated films at 54.12%, with O as the second highest at 29.07%. In contrast, the uncoated films had C as the main component, closely followed by that with O (45.19% and 43.34%, respectively). The amounts of the other elements were low. This result provides further evidence that eco-films, both coated and uncoated, contain inorganic mineral matter. It also highlights the highly heterogeneous nature of the specimens, consistent with the findings of previous research on eco-films.⁴⁴

Mechanical Properties. The elongation at break, tensile strength, tensile index, and modulus of elasticity of the coated JCC/TPU and uncoated JCC fabricated eco-films are presented in Figure 6. The results indicated that the elongation at break, tensile strength, tensile index, and modulus of elasticity of the eco-films increased significantly with the amount of JCC, and these properties were higher in the coated films than in the uncoated films. This increase can be attributed to higher breaking elongation properties and higher modulus of elasticity or increased film thickness. Overall, the uncoated films (JCC6, JCC8, and JCC10) exhibited tensile strength around 4.8–10.7 MPa, elongation at break around 66.7–77.1%, modulus of elasticity around 62.4–141.6 MPa, and tensile index around 38.07–39.6 N m/g. In contrast, the coated films (JCC6/TPU, JCC8/TPU, and JCC10/TPU) coated with TPU showed higher values for tensile strength (16.1–30.2 MPa), elongation at break (119.4–124.0%), modulus of elasticity (96.0–148.6 MPa), and tensile index (47.66–62.87 N m/g). For the coated JCC/TPU or uncoated JCC films, the elongation at break, tensile strength, tensile index, and modulus of elasticity all increased significantly ($p \leq 0.5$) with different thicknesses. According to previous research,⁵⁶ a higher amount of JCC was included to increase the strength, leading to improved strength properties of the fabricated films. The thickness of the film is not immediately considered in the tensile index calculation, even though film thickness affects the strength. If the density of the film is constant and the tensile index is related to the mass per unit area of the film and indirectly to the thickness, then the weight increases as the thickness increases. However, it was found that the eco-films created in this study had a higher tensile strength than standard LDPE (12.6–14.3 MPa).⁵⁷ An LDPE film was also analyzed for tensile strength, although the results are not displayed in Figure 6. The changes in elongation at break were consistently upward, suggesting that the isocyanate groups (NCO) in TPU and the (–OH) groups in cellulose contribute to local stabilization, leading to better mechanical properties.

Thickness and GSM. The eco-friendly non-woven films were manufactured using varying amounts of JCC (i.e., 6 g denoted as JCC6, 8 g as JCC8, and 10 g as JCC10), and all films were coated with TPU. The GSM of the coated and uncoated non-woven films increased with increasing JCC amounts, and thickness also increased proportionally with the increasing GSM of the films with the same diameter (i.e., GSM

and thickness exhibited a direct relationship; see Figure S4). However, due to heat-pressing, the thickness of the coated films decreased significantly compared to that of the uncoated ones. On the other hand, the thickness increase was consistent with increasing GSM (e.g., thickness = 0.15 mm at GSM = 101.58 for JCC6/TPU, thickness = 0.18 mm at GSM = 134.03 for JCC8/TPU, and thickness = 0.21 mm at GSM = 144.18 for JCC10/TPU). Nevertheless, the experiments on the films revealed that increased GSM thickness led to elevated tensile strength and biodegradability but decreased transparency and contact angle. This is because the higher amount of JCC confirmed the incorporation of numerous fibers into the matrix, which ultimately showed a good level of biodegradability, as pristine JCC is completely biodegradable.

Sessile Water Drop Contact Angle. The sessile water droplet contact angles on the surface of coated JCC6/TPU, JCC8/TPU, and JCC10/TPU and uncoated JCC6, JCC8, and JCC10 non-woven fabricated eco-films, TPU film, and an LDPE bag are presented in Figure 7. Figure 7a excellently illustrates the contact angle of sessile water droplets on coated JCC6/TPU, JCC8/TPU, and JCC10/TPU and uncoated JCC6, JCC8, and JCC10 films after 1 s, while Figure 7b displays the same for up to 20 min. The contact angle volume, indicative of the barrier to sessile water droplet penetration, increases with a higher contact angle. The coated non-woven fabricated films exhibited superior water resistance compared to the TPU film and the very thin LDPE bag. This enhancement is attributed to the increased crystallinity or thickness of the coated non-woven fabricated films, particularly in comparison to the exceedingly thin LDPE bag. The heightened crystallinity results from the reaction between the hydroxyl group (OH) of JCC and the isocyanate active group (NCO) in TPU under heat and pressure. Additionally, the thickness of the coated fabricated eco-films increased with the JCC content.

The uncoated fabricated eco-films (JCC6, JCC8, and JCC10) exhibited contact angles of 34.9°, 38.0°, and 40.2° (hydrophilic region), respectively, within the first second. However, after 1 s, the sessile water droplet was readily absorbed. In contrast, the coated JCC6/TPU, JCC8/TPU, and JCC10/TPU films initially had contact angles higher than 100° (e.g., 119.2°, 114.3°, and 108.4°), which gradually increased up to 30 s, stabilized (e.g., 121.9°, 115.8°, and 114.2°), and then slowly decreased. The coated films remained hydrophobic for about 600 s, after which the sessile water droplets gradually settled on the films' surface due to their thickness-dependent characteristics (e.g., 105.7°, 98.1°, and 68.6°). The hydrophobic or hydrophilic behavior of the films is influenced by an esterification reaction between the isocyanate active group (NCO) and the hydroxyl group of JCC, confirmed by FT-IR spectra, and influenced by the films' thickness properties.

The films were classified as hydrophilic (contact angle volumes between 0° and 90° ±), hydrophobic (contact angle volumes between 90°–180° ±), and lipophilic.⁴⁷ After 10 min, the contact angles of the coated films JCC6/TPU, JCC8/TPU, and JCC10/TPU (e.g., 106.4°, 104.8°, and 103.4°) were higher than 90° ±, indicating hydrophobic behavior. These values surpassed those of other coating films, such as CGT/PVA-EC (65°),⁵⁷ BP1-EC and WH1-EC (83.6°, 72.4°),⁵⁸ and 7% CGT film (46°).⁵⁴ Notably, the contact angle values for the JCC6/TPU and JCC8/TPU films remained above the hydrophobic level (i.e., 105.7° and 98.1°) up to 20 min, while that of the JCC10/TPU film dropped below the

hydrophilic level (i.e., 68.6°), indicating biodegradability. However, beyond 1200 s, the contact angles for the JCC6/TPU and JCC8/TPU films exceeded 90° ±, while that of the JCC10/TPU film remained below 90° ±. The hydrophobic or hydrophilic behavior is attributed to an esterification reaction between the isocyanate active group (NCO) and the hydroxyl group of JCC, as confirmed by FT-IR spectra, and is influenced by the film's thickness properties.⁵⁴ Therefore, the TPU coating on JCC non-woven eco-films provides resistance to sessile water droplets throughout the lifespan of the biopolymer films, making them suitable for specific packaging applications.

Air Permeability. Air permeability, defined as the air movement through uncoated and coated non-woven fabricated eco-films under specific air pressure conditions, was assessed in this study. In the uncoated JCC6, JCC8, and JCC10 non-woven fabricated eco-films, air permeability reduces with an increase in GSM and thickness (see Figure S6a). The CV% remains low despite an increase in CV% being attributed to the loose bonding of these films. Conversely, the air permeability of the coated JCC6/TPU, JCC8/TPU, and JCC10/TPU non-woven fabricated eco-films steadily decreases, reaching near-zero levels with increasing GSM and thickness (see Figure S6b). The CV% of air permeability, driven by high air pressure, exhibits an upward trend compared to uncoated films and decreases consistently depending on the GSM and thickness. The interlocking of JCC components in fabricating non-woven eco-packaging contributes to the film's ability to resist air pressure.⁵⁹ Therefore, GSM and thickness are crucial in determining air pressure levels in coated and uncoated eco-films. The investigation into air permeability variation reveals significant numerical impacts of GSM and thickness within the studied ratio of values for the coated JCC6/TPU, JCC8/TPU, and JCC10/TPU and uncoated JCC6, JCC8, and JCC10 non-woven fabricated eco-films.

Biodegradability of Eco-Films. The weight loss resulting from the biodegradation of the coated JCC/TPU and uncoated JCC non-woven fabricated films over 120 days is depicted in Figure 8a. According to published data,⁵⁹ substituting OH groups may negatively impact the biodegradation duration of the coated and uncoated fabricated films. While some OH group replacement occurred in the coated JCC/TPU non-woven fabricated films, this study found an insignificant effect on the films' biodegradation period. Conversely, OH group replacement did not occur in the uncoated JCC non-woven fabricated films.

After a few days, the weight loss ratio increased for both the coated and uncoated fabricated films. In the case of the coated fabricated films, the investigation revealed weight loss percentages ranging from 7.62% to 14% after 20 days, 16.39% to 23.33% after 40 days, 21.44% to 29.18% after 60 days, 37.15% to 39.21% after 80 days, 47.13% to 56.91% after 100 days, and 51.78% to 62.35% after 120 days. For the uncoated fabricated films, weight loss percentages were between 28.44% and 37.45% after 20 days, between 83.59% and 90.01% after 40 days, and 100% around 60 days, indicating complete weight loss during the biodegradation period. An increase in the amount of JCC corresponds to an increase in the weight loss of the suppressed fabricated films. This outcome aligns with the biodegradation observed in ref 54, where fabricated films from cotton gin trash lost 43–46% of their weight in 30 days. Due to the hydrophilic nature of JCC, it attracts water molecules from the soil, which, in turn, attract

degrading enzymes. This cycle continues until the bonds of JCC, CMC, and TPU are torn, leading to the breakdown of the films, as cellulosic materials absorb water.

Another aspect of the experiment, illustrated in Figure 8b, demonstrated that LDPE, when burned, transformed into harmful solid particles without being destroyed. In contrast, the coated fabricated films burned to ashes, potentially enhancing soil fertility. The fabricated films have the potential to be converted into conventional fuel after use, posing a minimal burden on the environment and offering a threefold benefit.

Table 5 shows the comparison among different eco-films made with cellulose-based materials. The overall mechanical properties of the JC films were better than those of the other films except for the Young's modulus. On the other hand, the biodegradability of the JC eco-films was slightly lower than that of other films like hemp and seaweed. This is because the JC films are made with waste materials and possess lower strength than the others. But the overall properties compared to the others are in an acceptable limit to claim the JC films as eco-films for packing materials.

CONCLUSIONS

This study introduces a groundbreaking example of an exceptionally water-resistant and environmentally friendly film crafted from pure jute caddis cellulose (JCC). The JCC/TPU eco-film emerges as a promising alternative to ecologically harmful plastics commonly employed in flexible packaging, spanning applications such as in the food industry, medicine, household items, and more. The film's biodegradability, solubility restriction, and molecular weight and the linearity of the coating's chemical structure collectively influenced the polymerization process. The film properties investigated in this study were notably affected by the quantity of JCC incorporated into the film. Total flexibility, demonstrated by a folding tolerance exceeding 100, was achieved by blending 5%, 7.5%, and 9.5% TPU with 6, 8, and 10 g of JCC, respectively. While the modulus of the coated films (148.6 MPa) was lower than that of LDPE (213.5 MPa), the tensile strength (ranging from 16.1 to 32.2 MPa) surpassed that of LDPE (12.6–14.3 MPa). The air permeability of the coated film exhibited a substantial decrease, ranging from 95.95% to 99.38%, compared to that of the uncoated film. The presence of TPU positively contributed to this decrease. After being coated with TPU, the films (JCC6/TPU, JCC8/TPU, and JCC10/TPU) demonstrated resistance to sessile water droplets for at least 20 min, maintaining minimum contact angles of 105.7°, 98.1°, and 68.6°, respectively. In the visible light region, these films exhibited light transmission ranging from 51.99% to 60.05%. In conclusion, the JCC/TPU eco-film explored in this research holds significant potential for diverse everyday applications. Future endeavors will focus on monitoring research and implementing extrusion equipment to enhance the consistency and efficiency of the bulk production of JCC/TPU eco-films.

ASSOCIATED CONTENT

Data Availability Statement

The data underlying this study will be provided upon request.

Supporting Information

The Supporting Information is available free of charge at <https://pubs.acs.org/doi/10.1021/acssusresmgmt.3c00123>.

Optical transmittance of coated and uncoated eco-films, cross-sectional analysis of JCC/TPU-coated film, cleaning process of eco-film, GSM and thickness values of the coated and uncoated fabricated eco-films, elemental analysis of the coated and uncoated eco-films, and air permeability and CV% of the coated and uncoated films (PDF)

AUTHOR INFORMATION

Corresponding Authors

M Mahbulul Bashar – Department of Textile Engineering, Mawlana Bhashani Science and Technology University, Tangail 1902, Bangladesh; orcid.org/0000-0001-8054-809X; Email: bashar.te@mbstu.ac.bd

Tarikul Islam – Department of Textiles, Merchandising, and Interiors, University of Georgia, Athens, Georgia 30602, United States; Department of Textile Engineering, Jashore University of Science and Technology, Jashore 7408, Bangladesh; orcid.org/0000-0002-3106-378X; Email: tarikul@uga.edu, mti@just.edu.bd

Authors

Khairul Islam – Department of Textile Engineering, Mawlana Bhashani Science and Technology University, Tangail 1902, Bangladesh; Bangladesh Jute Mills Corporation, Ministry of Textiles and Jute, Dhaka 1000, Bangladesh

Md. Nura Alam Shiddique – Department of Textile Engineering, World University of Bangladesh, Dhaka 1230, Bangladesh

Manindra Nath Roy – Department of Textile Engineering, Mawlana Bhashani Science and Technology University, Tangail 1902, Bangladesh; Department of Textile Engineering, Northern University of Bangladesh, Dhaka 1230, Bangladesh

Md Fahimuzzaman – Department of Textile Engineering, Mawlana Bhashani Science and Technology University, Tangail 1902, Bangladesh

Md. Azharul Islam – Department of Textile Engineering, Mawlana Bhashani Science and Technology University, Tangail 1902, Bangladesh

Mubarak A. Khan – Bangladesh Jute Mills Corporation, Ministry of Textiles and Jute, Dhaka 1000, Bangladesh

Complete contact information is available at:

<https://pubs.acs.org/10.1021/acssusresmgmt.3c00123>

Author Contributions

Conceptualization: K.I., and M.M.B.; Methodology: K.I., T.I., and M.M.B.; Formal analysis: K.I., T.I., and M.M.B.; Investigation: K.I., T.I., M.M.B., and M.A.K.; Validation: K.I., T.I., M.N.A.S., M.N.R., M.F., M.A.I., M.M.B., and M.A.K.; Resources: K.I., and M.M.B.; Visualization: K.I., M.N.A.S., M.N.R., M.F., M.A.I., and M.M.B.; Supervision: M.M.B., and M.A.K.; Original draft: K.I.; Writing, review, and editing: K.I., T.I., and M.M.B.; All authors contributed to the article and approved the submitted version.

Notes

The authors declare no competing financial interest.

ACKNOWLEDGMENTS

The authors acknowledge the support from the Department of Textile Engineering, Mawlana Bhashani Science and Technol-

ogy University, Bangladesh, and Sonali Bag Project, BJMC, and the Ministry of Textiles and Jute, Bangladesh.

REFERENCES

- (1) Lebreton, L.; Andrady, A. Future Scenarios of Global Plastic Waste Generation and Disposal. *Palgrave Commun.* **2019**, *5* (1), 6.
- (2) Geyer, R.; Jambeck, J. R.; Law, K. L. Production, Use, and Fate of All Plastics Ever Made. *Sci. Adv.* **2017**, *3* (7), e1700782 DOI: 10.1126/sciadv.1700782.
- (3) Xing, C.; Cai, H.; Kang, D.; Sun, W. Photothermal Catalysis: An Emerging Green Approach to Upcycling Plastic Waste. *Advanced Energy and Sustainability Research* **2023**, *4* (10), 2300015 DOI: 10.1002/aesr.202300015.
- (4) Abdullah, Z. W.; Dong, Y. Biodegradable and Water Resistant Poly(Vinyl Alcohol (PVA)/Starch (ST)/Glycerol (GL)/Halloysite Nanotube (HNT) Nanocomposite Films for Sustainable Food Packaging. *Front Mater.* **2019**, *6*, 58 DOI: 10.3389/fmats.2019.00058.
- (5) Mi, H.-Y.; Salick, M. R.; Jing, X.; Jacques, B. R.; Crone, W. C.; Peng, X.-F.; Turng, L.-S. Characterization of Thermoplastic Polyurethane/Poly(lactic Acid (TPU/PLA) Tissue Engineering Scaffolds Fabricated by Microcellular Injection Molding. *Materials Science and Engineering: C* **2013**, *33* (8), 4767–4776.
- (6) Li, H.; Shi, H.; He, Y.; Fei, X.; Peng, L. Preparation and Characterization of Carboxymethyl Cellulose-Based Composite Films Reinforced by Cellulose Nanocrystals Derived from Pea Hull Waste for Food Packaging Applications. *Int. J. Biol. Macromol.* **2020**, *164*, 4104–4112.
- (7) Ma, X.; Chang, P. R.; Yu, J. Properties of Biodegradable Thermoplastic Pea Starch/Carboxymethyl Cellulose and Pea Starch/Microcrystalline Cellulose Composites. *Carbohydr. Polym.* **2008**, *72* (3), 369–375.
- (8) Salem, T. F.; Tirkes, S.; Akar, A. O.; Tayfun, U. Enhancement of Mechanical, Thermal and Water Uptake Performance of TPU/Jute Fiber Green Composites via Chemical Treatments on Fiber Surface. *e-Polymers* **2020**, *20* (1), 133–143.
- (9) Chen, W.-H.; Wang, C.-W.; Ong, H. C.; Show, P. L.; Hsieh, T.-H. Torrefaction, Pyrolysis and Two-Stage Thermodegradation of Hemicellulose. *Cellulose and Lignin. Fuel* **2019**, *258*, No. 116168.
- (10) Nayak, L.; Roy, A. Utilisation of Jute By-Products: A Review. *Agricultural Reviews* **2011**, *32* (1), 63–69.
- (11) Basak, M. K.; Chanda, S.; Bhaduri, S. K.; Mondal, S. B.; Nandi, R. Recycling of Jute Waste for Edible Mushroom Production. *Ind. Crops Prod* **1996**, *5* (3), 173–176.
- (12) Masoodi, R.; Pillai, K. M. A Study on Moisture Absorption and Swelling in Bio-Based Jute-Epoxy Composites. *Journal of Reinforced Plastics and Composites* **2012**, *31* (5), 285–294.
- (13) Ghosh, S. K.; Bhattacharyya, R.; Mondal, M. M. A Review on Jute Geotextile-Part 1. *IJRET* **2014**, *03* (2), 378–386.
- (14) Majumder, A.; Samajpati, S.; Ganguly, P. K.; Sardar, D.; Das Gupta, P. C. Swelling of Jute: Heterogeneity of Crimp Formation. *Text. Res. J.* **1980**, *50* (9), 575–578.
- (15) Roy, G.; Saha, S. C. Development of Digital Moisture Meter for Jute Fibre and Its Products. *Indian Journal of Fibre & Textile Research* **2011**, *36*, 178–182.
- (16) Chakrabarti, S. K.; Saha, S. G.; Basu, S.; Mukhopadhyay, G.; De, S.; Sanyal, P.; Ray, P. Energy Efficient Novel Sizing of Jute Yarns. *Journal of Natural Fibers* **2016**, *13* (2), 178–191.
- (17) Sundarraj, A. A.; Ranganathan, T. V. A Review on Cellulose and Its Utilization from Agro-Industrial Waste. *Drug Invention Today* **2018**, *10* (1), 89–94.
- (18) Gabrielli, V.; Frascioni, M. Cellulose-Based Functional Materials for Sensing. *Chemosensors* **2022**, *10* (9), 352.
- (19) Olugbenga, O.; Labunmi, L.; Bodunde, O. Microcrystalline Cellulose from Plant Wastes through Sodium Hydroxide-Anthraquinone-Ethanol Pulping. *BioResources* **2014**, *9* (4), 6166–6192.
- (20) Nasibi, S.; Nargesi khoramabadi, H.; Arefian, M.; Hojjati, M.; Tajzad, I.; Mokhtarzade, A.; Mazhar, M.; Jamavari, A. A Review of Poly(vinyl Alcohol / Carboxy Methyl Cellulose (PVA/CMC) Composites for Various Applications. *Journal of Composites and Compounds* **2020**, *2* (3), 68–75.
- (21) Kamthai, S.; Magaraphan, R. Mechanical and Barrier Properties of Spray Dried Carboxymethyl Cellulose (CMC) Film from Bleached Bagasse Pulp. *Ind. Crops Prod* **2017**, *109*, 753–761.
- (22) Orasugh, J. T.; Saha, N. R.; Rana, D.; Sarkar, G.; Mollick, Md. M. R.; Chattopadhyay, A.; Mitra, B. C.; Mondal, D.; Ghosh, S. K.; Chattopadhyay, D. Jute Cellulose Nano-Fibrils/Hydroxypropylmethylcellulose Nanocomposite: A Novel Material with Potential for Application in Packaging and Transdermal Drug Delivery System. *Ind. Crops Prod* **2018**, *112*, 633–643.
- (23) Barba, C.; Montané, D.; Rinaudo, M.; Farriol, X. Synthesis and Characterization of Carboxymethylcelluloses (CMC) from Non-Wood Fibers I. Accessibility of Cellulose Fibers and CMC Synthesis. *Cellulose* **2002**, *9*, 319–326.
- (24) Thivya, P.; Akalya, S.; Sinija, V. R. A Comprehensive Review on Cellulose-Based Hydrogel and Its Potential Application in the Food Industry. *Applied Food Research* **2022**, *2* (2), No. 100161.
- (25) Jiang, Z.; Ngai, T. Recent Advances in Chemically Modified Cellulose and Its Derivatives for Food Packaging Applications: A Review. *Polymers (Basel)* **2022**, *14* (8), 1533.
- (26) Yao, Y.; Sun, Z.; Li, X.; Tang, Z.; Li, X.; Morrell, J. J.; Liu, Y.; Li, C.; Luo, Z. Effects of Raw Material Source on the Properties of CMC Composite Films. *Polymers (Basel)* **2022**, *14* (1), 32.
- (27) Kumar, R.; Sharma, R. Kr.; Singh, A. P. Grafted Cellulose: A Bio-Based Polymer for Durable Applications. *Polym. Bull.* **2018**, *75* (5), 2213–2242.
- (28) Lan, W.; He, L.; Liu, Y. Preparation and Properties of Sodium Carboxymethyl Cellulose/Sodium Alginate/Chitosan Composite Film. *Coatings* **2018**, *8* (8), 291.
- (29) Frick, A.; Rochman, A. Characterization of TPU-Elastomers by Thermal Analysis (DSC). *Polym. Test* **2004**, *23* (4), 413–417.
- (30) Tayfun, U.; Dogan, M.; Bayramli, E. Influence of Surface Modifications of Flax Fiber on Mechanical and Flow Properties of Thermoplastic Polyurethane Based Eco-Composites. *Journal of Natural Fibers* **2016**, *13* (3), 309–320.
- (31) Herrera, M.; Matuschek, G.; Kettrup, A. Thermal Degradation of Thermoplastic Polyurethane Elastomers (TPU) Based on MDI. *Polym. Degrad Stab* **2002**, *78* (2), 323–331.
- (32) Noor Azammi, A. M.; Sapuan, S. M.; Ishak, M. R.; Sultan, M. T. H. Mechanical and Thermal Properties of Kenaf Reinforced Thermoplastic Polyurethane (TPU)-Natural Rubber (NR) Composites. *Fibers Polym.* **2018**, *19* (2), 446–451.
- (33) El-Shekeil, Y. A.; Sapuan, S. M.; Khalina, A.; Zainudin, E. S.; Al-Shuja'a, O. M. Effect of Alkali Treatment on Mechanical and Thermal Properties of Kenaf Fiber-Reinforced Thermoplastic Polyurethane Composite. *J. Therm Anal Calorim* **2012**, *109* (3), 1435–1443.
- (34) Rozman, H. D.; Tay, G. S. The Effects of NCO/OH Ratio on Propylene Oxide-modified Oil Palm Empty Fruit Bunch-based Polyurethane Composites. *J. Appl. Polym. Sci.* **2008**, *110* (6), 3647–3654.
- (35) Bakare, I.O.; Okieimen, F.E.; Pavithran, C.; Abdul Khalil, H.P.S.; Brahmakumar, M. Mechanical and Thermal Properties of Sisal Fiber-Reinforced Rubber Seed Oil-Based Polyurethane Composites. *Mater. Des.* **2010**, *31* (9), 4274–4280.
- (36) Wilberforce, S.; Hashemi, S. Effect of Fibre Concentration, Strain Rate and Weldline on Mechanical Properties of Injection-Moulded Short Glass Fibre Reinforced Thermoplastic Polyurethane. *J. Mater. Sci.* **2009**, *44* (5), 1333–1343.
- (37) Vajrasthira, C.; Amornsakchai, T.; Bualek-Limcharoen, S. Fiber-Matrix Interactions in Aramid-short-fiber-reinforced Thermoplastic Polyurethane Composites. *J. Appl. Polym. Sci.* **2003**, *87* (7), 1059–1067.
- (38) El-Shekeil, Y. A.; Sapuan, S. M.; Abdan, K.; Zainudin, E. S. Influence of Fiber Content on the Mechanical and Thermal Properties of Kenaf Fiber Reinforced Thermoplastic Polyurethane Composites. *Mater. Des.* **2012**, *40*, 299–303.
- (39) Ghanbarzadeh, B.; Almasi, H.; Entezami, A. A. Physical Properties of Edible Modified Starch/Carboxymethyl Cellulose Films.

Innovative Food Science & Emerging Technologies **2010**, *11* (4), 697–702.

(40) Ibrahim, M. M.; Koschella, A.; Kadry, G.; Heinze, T. Evaluation of Cellulose and Carboxymethyl Cellulose/Poly(Vinyl Alcohol) Membranes. *Carbohydr. Polym.* **2013**, *95* (1), 414–420.

(41) Bashar, M. M.; Ohara, H.; Zhu, H.; Yamamoto, S.; Matsui, J.; Miyashita, T.; Mitsuiishi, M. Cellulose Nanofiber Nanosheet Multilayers by the Langmuir–Blodgett Technique. *Langmuir* **2019**, *35* (24), 8052–8059.

(42) Sarkar, M.; Nayeem, J.; Popy, R. S.; Quadery, A. H.; Sarwar Jahan, M. Dissolving Pulp from Jute Wastes. *Bioresour Technol. Rep* **2018**, *4*, 96–100.

(43) Hassan, M. M.; Saifullah, K. Ultrasound-Assisted Pre-Treatment and Dyeing of Jute Fabrics with Reactive and Basic Dyes. *Ultrason Sonochem* **2018**, *40*, 488–496.

(44) Haque, A. N. M. A.; Remadevi, R.; Wang, X.; Naebe, M. Mechanically Milled Powder from Cotton Gin Trash for Diverse Applications. *Powder Technol.* **2020**, *361*, 679–686.

(45) Haque, A. N. M. A.; Remadevi, R.; Wang, X.; Naebe, M. Absorption Properties of Fabricated Film from Cotton Gin Trash. *Mater. Today Proc.* **2020**, *31* (xxxx), S221–S226.

(46) Mollick, S.; Islam, T.; Miah, M. R.; Riad, M. M. H.; Chakrabarty, T.; Hossen, M. T.; Islam, M. T. Development of Antibacterial Cotton Fabric Utilizing Microencapsulation Technique from Dragon Fruit Peel Extract. *Fibers Polym.* **2023**, *24*, 3937–3945.

(47) Mascarenhas, A. R. P.; Scatolino, M. V.; Santos, A. d. A. d.; Norcino, L. B.; Duarte, P. J.; Melo, R. R. d.; Dias, M. C.; Faria, C. E. T. d.; Mendonça, M. C.; Tonoli, G. H. D. Hydroxypropyl Methylcellulose Films Reinforced with Cellulose Micro/Nanofibrils: Study of Physical, Optical, Surface, Barrier and Mechanical Properties. *Nord Pulp Paper Res. J.* **2022**, *37* (2), 366–384.

(48) Yang, D.; Peng, X.; Zhong, L.; Cao, X.; Chen, W.; Zhang, X.; Liu, S.; Sun, R. Green Films from Renewable Resources: Properties of Epoxidized Soybean Oil Plasticized Ethyl Cellulose Films. *Carbohydr. Polym.* **2014**, *103*, 198–206.

(49) Popescu, C.-M.; Popescu, M.-C.; Singurel, G.; Vasile, C.; Argyropoulos, D. S.; Willfor, S. Spectral Characterization of Eucalyptus Wood. *Appl. Spectrosc.* **2007**, *61* (11), 1168–1177.

(50) Plácido, J.; Imam, T.; Capareda, S. Evaluation of Ligninolytic Enzymes, Ultrasonication and Liquid Hot Water as Pretreatments for Bioethanol Production from Cotton Gin Trash. *Bioresour Technol.* **2013**, *139*, 203–208.

(51) Oh, J.; Kim, Y. K.; Hwang, S.-H.; Kim, H.-C.; Jung, J.-H.; Jeon, C.-H.; Kim, J.; Lim, S. K. Preparation of Side-By-Side Bicomponent Fibers Using Bio Polyol Based Thermoplastic Polyurethane (TPU) and TPU/Poly(lactic Acid) Blends. *Fibers* **2022**, *10* (11), 95.

(52) Pandey, K. K.; Pitman, A. J. FTIR Studies of the Changes in Wood Chemistry Following Decay by Brown-Rot and White-Rot Fungi. *Int. Biodeterior Biodegradation* **2003**, *52* (3), 151–160.

(53) Hasan, M. Z.; Arafat, Y.; Bashar, M. M.; Niloy, M. N. N.; Islam, M. I.; Khandaker, S.; Chowdhury, A. M. S. Poly-(Vinyl Alcohol) Composite Films Reinforced with Carboxylated Functional Microcrystalline Cellulose from Jute Fiber. *Composites and Advanced Materials* **2022**, *31*, 1 DOI: [10.1177/26349833221103888](https://doi.org/10.1177/26349833221103888).

(54) Haque, A. N. M. A.; Remadevi, R.; Wang, X.; Naebe, M. Physicochemical Properties of Film Fabricated from Cotton Gin Trash. *Mater. Chem. Phys.* **2020**, *239*, No. 122009.

(55) Cai, Z.; Remadevi, R.; Al Faruque, M. A.; Setty, M.; Fan, L.; Haque, A. N. M. A.; Naebe, M. Fabrication of a Cost-Effective Lemongrass (*Cymbopogon Citratus*) Membrane with Antibacterial Activity for Dye Removal. *RSC Adv.* **2019**, *9* (58), 34076–34085.

(56) Syduzzaman, M.; Al Faruque, M. A.; Bilisik, K.; Naebe, M. Plant-Based Natural Fibre Reinforced Composites: A Review on Fabrication, Properties and Applications. *Coatings* **2020**, *10* (10), 973.

(57) Haque, A. N. M. A.; Naebe, M. Flexible Water-Resistant Semi-Transparent Cotton Gin Trash/Poly (Vinyl Alcohol) Bio-Plastic for Packaging Application: Effect of Plasticisers on Physicochemical Properties. *J. Clean Prod* **2021**, *303*, No. 126983.

(58) Hosen, M. D.; Hossain, M. S.; Islam, M. A.; Haque, A. N. M. A.; Naebe, M. Utilisation of Natural Wastes: Water-Resistant Semi-Transparent Paper for Food Packaging. *J. Clean Prod* **2022**, *364*, No. 132665.

(59) Pivsa-Art, S.; Roungpaisan, N.; Malimat, M.; Pivsa-Art, W. Sound Absorbing Panels from Poly(Lactic Acid) Non-Woven Fabric and Natural Fibers. *Suan Sunandha Science and Technology Journal* **2022**, *9* (2), 79–86.

(60) Nabels-Sneiders, M.; Platnieks, O.; Grase, L.; Gaidukovs, S. Lamination of Cast Hemp Paper with Bio-Based Plastics for Sustainable Packaging: Structure-Thermomechanical Properties Relationship and Biodegradation Studies. *Journal of Composites Science* **2022**, *6* (9), 246.

(61) Hasan, M.; Lai, T. K.; Gopakumar, D. A.; Jawaid, M.; Owolabi, F. A. T.; Mistar, E. M.; Alfatah, T.; Noriman, N. Z.; Haafiz, M. K. M.; Abdul Khalil, H. P. S. Micro Crystalline Bamboo Cellulose Based Seaweed Biodegradable Composite Films for Sustainable Packaging Material. *J. Polym. Environ* **2019**, *27* (7), 1602–1612.